

Basic Mechanisms of Fluting Formation and Retention in Paper

Artem Kulachenko, Per A Gradin and Tetsu Uesaka

FSCN

Fibre Science and Communication Network
- ett skogsindustriellt forskningsprogram vid Mittuniversitetet

BASIC MECHANISMS OF FLUTING FORMATION AND RETENTION IN PAPER

Artem Kulachenko^{*}, Per Gradin and Tetsu Uesaka

Fibre Science and Communication Network (FSCN)

Mid Sweden University

85170, Sundsvall, Sweden

ABSTRACT

Out-of-plane deformations of paper, such as fluting, significantly deteriorate the quality of a printed product. There are several explanations of fluting presented in the literature but there is no unanimously accepted theory regarding fluting formation and retention which is consistent with all field observations. This paper first reviews the existing theories and proposes a mechanism that might give an answer to most of the questions regarding fluting. The fluting formation has been considered as a post-buckling phenomenon which has been analysed with the help of the finite element method. Fluting retention has been modelled by introducing an ink layer over the paper surface with the ink stiffness estimated from experimental results. The impact of fast drying on fluting has been assessed numerically and experimentally. The result of the study suggests that fluting occurs due to small-scale hygro-strain variations, which in turn are caused by the moisture variations created during fast convection (through-air) drying. The result also showed that ink stiffening alone cannot explain the fluting amplitudes observed in practice, but that high drying temperatures promote inelastic (irreversible) deformations in paper and this may itself preserve fluting.

Keywords: fluting, cockling, moisture variations, fibre orientation.

^{*} Corresponding author. Tel.: +46-60-148996; Fax: +46-60-148820
E-mail address: Artem.Kulachenko@miun.se.

CONTENTS

ABSTRACT.....	1
1. INTRODUCTION.....	3
1.1 Literature survey	3
2. NUMERICAL ANALYSIS OF PAPER WITH MICRO SCALE STRAIN VARIATIONS	7
3. EXPERIMENTAL MEASUREMENTS OF INK STIFFNESS	8
4. FORMATION OF FLUTING.....	9
4.1 Factors affecting fluting: Parametric studies.....	9
4.2 Effect of fibre orientation	13
4.3 Effects of drying non-uniformity	17
4.4 Visualization of air permeation variation in paper	18
5. FLUTING RETENTION.....	20
5.1 Numerical analysis.....	20
5.2 Experimental analysis	22
5.3 Effect of temperature on residual deformation in paper	25
6. CONCLUSION	27
ACKNOWLEDGEMENTS.....	27
APPENDIX: ESTIMATE OF INK STIFFNESS BY DROOP TEST.....	28
REFERENCES.....	31

1. INTRODUCTION

Fluting of paper is a phenomenon occurring during the heatset offset printing process. It manifests itself through wavy wrinkles oriented in the length direction (machine direction, MD) of the web. It often appears on paper in connection with printing operations involving two-sided, heavy ink coverage (Fig. 1).



Fig. 1. A typical fluting appearance

Fluting occurs only in web-fed, heatset offset printing. This type of printing covers most of the *higher quality* printing market. Fluting usually appears in the final product with the wavelength of 1-2cm. Because of its appearance it seriously deteriorates the perceived printing quality.

1.1 Literature survey

Most of the articles regarding fluting were reviewed by MacPhee et al. (2000) and more recently by Kulachenko et al. (2006). Typically several topics are discussed in relations to fluting such as tension, drying temperature, presence of ink etc. We will present the relevant literature findings according to these topics.

1.1.1 Tension and heat

In the web-fed heatset offset printing process, the paper web is subjected to tension. Ink and sometimes water is applied onto the paper web in the printing stations and then dried in the dryer. It is unanimously supported that both tension and heat are required to create fluting (MacPhee et al., 2000). Paper may wrinkle by tension only but it was noted that applying heat, in addition to tension, creates a sharper and narrower fluting pattern than tension alone (Hung, 1984). On the other hand, upon applying heat only, the out-of-plane distortions of paper do not have the wavy fluting appearance (Strong, 1984).

The web tension in the dryer usually varies from 250 to 500N/m (Falter and Schmitt, 1987). Hung (1984) showed that a thin web may experience fluting upon high intensity drying even at a low tension (100N/m and less). Falter and Schmitt (1987) reported that the web tension could not practically be decreased to the level where the fluting is acceptable.

The effects of web tension on fluting are not clear from the literature. Higher tension is often found to worsen fluting but for some papers, application of very high tension (900N/m)

produced less fluting (Strong, 1984a). Within a limited range of change in tension (a 17% decrease) no discernible effect was observed on fluting amplitude (MacPhee et al., 2000).

Fluting appears in the final product if web is heated to a certain high temperature (Mochizuki and Aoyama, 1981; MacPhee et al., 2000) or when air impingement velocity reaches a threshold limit (Mochizuki and Aoyama, 1981). However the effects of dryer configuration reported in the literature are not consistent. Strong (1984b) reported that press dryer configuration does not affect fluting (three manufactures, all lengths, including direct flame and high velocity hot air, were tested). Contrarily, MacPhee et al. (2000) found that open flame (impingement) dryers generally did not have a fluting problem. It may be interpreted that printing presses equipped with such open flame dryers are usually run at lower speeds and with moderate drying rates. However, Strong (1984b) did not find the web velocity to be a fluting factor. MacPhee et al. (2000) reported that longer residence time in the dryer resulted in an increase in fluting amplitudes.

Summarizing this subsection, we may say that the effect of tension and the drying method on fluting has not been clarified in the literature.

1.1.2 Moisture

Paper may take up and lose moisture during the printing process causing considerable hygroexpansion or shrinkage in paper.

During *printing*, MacPhee et al. (2000) found that the amount of moisture applied has negligible effect on fluting amplitudes. Printing with waterless plates and inks still caused fluting, in some cases even worse fluting.

During *drying*, Strong (1984a,b) did not find any relation between moisture loss and fluting. The moisture after printing varied from 0.1% to 5.4%. Measurements done by Falter and Schmitt (1987) showed that moisture can be completely lost from the paper during convection drying. The measured moisture content after the dryer was as low as 0.3%.

Contrary to what is shown in Strong's study (1984a,b), MacPhee et al (2000) showed that fluting amplitudes *decreased* by one third as the level of moisture in the paper before printing was reduced from 5% to 2.5%. Mochizuki and Aoyama (1982) reported that increasing recycling of air used in the convection dryer gave an improvement. It was attributed to decreased water evaporation from the paper.

Waech and Sze (1996) found that the fluting tendency is largely a function of the paper coating formulation: less absorbent coating flutes less. (However, it was noted that in spite of decreasing ink absorption, calendering (smoothing paper by compression) increased fluting tendency, i.e. highly calendered paper was more prone to flute.) Finally, Hirabayashi et al. (2005) showed that decreasing the moisture losses during drying to the minimum (by specially designed coating layer) may efficiently eliminate fluting.

In summary, the effects of moisture change are not consistently explained in the literature.

1.1.3 Basis weight (paper thickness)

Strong (1984a,b) found a general relationship between the width of the flutes and the basis weight: the flutes became wider as the paper basis weight increased. MacPhee et al. (2000) also reported that increasing basic weights increased the fluting wavelength but the fluting amplitude was not greatly affected by the basis weight. This observation is widely supported in the printing community.

1.1.4 Direction of paper grain

Owing to the manufacturing process, paper exhibits orthotropic properties. This is due to the fact that during paper forming fibres orient in the longitudinal direction of the roll (machine direction, MD). Therefore, the elastic stiffness in the MD is usually 3 times larger than that in the width direction (cross machine direction, CD). In addition, the hygroexpansion coefficient of paper in the CD is usually 3 times larger than in the MD. So if fluting is driven by hygro-strains, changing the direction of paper grain increases the critical moisture change, needed to initiate fluting, approximately by a factor of 9.

To examine the effect of direction of paper grain MacPhee et al. (2000) created a long spliced web with the grain in the cross direction (CD). When printed on, such web did not show typical fluting, but had a random out-of-plane distortion (called “cockles”), which disappeared after several hours.

1.1.5 Paper uniformity (formation) and initial defects

Paper structure is naturally non-uniform. Variations in density and thickness in paper can be seen by the naked eye. Such variations are the result of non-uniform *fibre mass distribution* (called “formation”). Falter and Schmitt (1987) found no correlation between formation and fluting. Some paper samples with uneven formation had a low waviness and vice versa. Strong (1984a,b) noted that most of the papers which showed fluting were free of any typical defects (streaks, ropes, etc).

1.1.6 Mechanism of fluting formation and retention

Two mechanisms have been proposed for fluting in the literature. Habeger (1993) explained fluting as tension wrinkles which were retained due to ink solidification. Fluting wavelength was estimated with the help of linear buckling theory. It was concluded that the observed fluting wavelengths should occur only in *sine wave* dryers where the web is subjected to airflow from both sides and the web takes a sinusoidal form. MacPhee et al. (2000), however, showed that fluting wavelength after “flat”-dryers was actually *similar* to that found in sine wave dryers.

Hirabayashi et al. (1998) proposed a mechanism of fluting formation based on differential shrinkage between image and non-image areas (Fig. 2). The authors postulated that image areas lose less moisture during drying as the ink layer prevents moisture from evaporation. (The presence of such difference in moisture loss was later experimentally confirmed by Simmons et al. (2001).) The fluting wavelength was reported to be dependent on the dimensions of the inked area. Fluting decreased with printing image length. It was opposite to the results reported by Mochizuki and Aoyama (1982), for example, who observed an increase in fluting with the length of printing area.

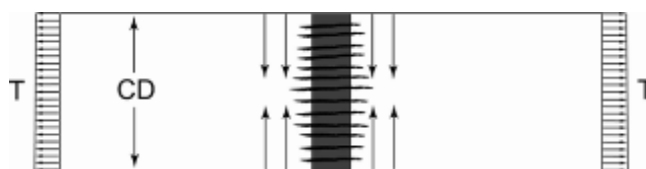


Fig. 2. Wrinkling due to differential shrinkage (image area is dark)

Coffin (2003) used the theory proposed by Hirabayashi et al. (1998) to predict the wavelength of fluting. Coffin (2003) showed that with this theory, tension is an important factor determining the fluting wavelengths. According to Coffin (2003) the tension required for fluting wavelength to be in the range of 1-2cm was estimated to be rather high, about 1000N/m. It was noted, however, that changes in stiffness caused by moisture changes during printing and drying cannot be accounted for in the linear buckling analysis used in the study.

MacPhee et al. (2000) showed that for light-weight coated (LWC) papers (60 g/m^2) fluting occurred both in image areas and in wide gutter with zero ink coverage. Fluting in the gutter relaxed to some extent, however. For LWC papers, wrinkles before the dryer bore no resemblance (in terms of wavelengths) to the wrinkles observed beyond the dryer, whereas for supercalendered (SC) paper, the appearance of wrinkles before and after the dryer was the same and resembled the fluting in the final products. Summarizing this, MacPhee et al. (2000) concluded that neither of these two theories consistently explains fluting.

Strong (1984a,b) showed that fluting amplitudes increased in high density prints especially on both-side printed areas. MacPhee et al. (2000) also showed that increasing ink film thickness increased fluting, eventually it reached a plateau. Mochizuki and Aoyama (1982) observed a significant relaxation of fluting amplitudes in the image area cut out of the sheet. This observation was not reproduced by Strong (1984b), i.e. fluting was just as permanent in cut image areas.

Strong (1984b) found that paper bending stiffness in the image areas is 25% higher than in non-image areas. Based on this data, Habeger (1993) and Hirabayashi et al. (1998) attributed fluting retention to ink solidification. Contrary to these results Hung (1984) showed that changes in paper stiffness due to ink solidification after drying is negligibly small. Furthermore, Hung (1984) came to the conclusion that the presence of ink is not necessary for fluting formation or for fluting retention. Hung (1984) explained fluting retention by intense heating. A more pronounced fluting pattern in the image areas was explained by the optical effect and more heat transfer to these areas during drying. The speculation that image areas attract more heat was confirmed by MacPhee et al. (2000), who showed that the temperature in the image areas right after the first chill roll ranged from 50°C to 60°C whereas in non-image areas it was approximately 35°C .

Clearly these two existing theories for fluting are not consistent with the observations published in the literature. Part of the reason lies in the fact that the two theories are based on linear-buckling analyses, whereas fluting is, in essence, a post-buckling phenomenon.

Kulachenko et al. (2005) performed geometrically non-linear, large scale post-buckling analyses. A lay-out with image and non-image areas was used in the analyses. Results showed that when the paper web was flat before printing, fluting patterns after printing, drying and moisture recovery consistently had higher wavelength (5-10cm) than those typically observed in fluted samples. In other words, the macroscopic loading and boundary conditions, as typically applied in the web-fed heatset offset printing process, cannot explain fluting in the printed sheet.

Summarizing the results of this literature survey, the mechanism of fluting formation and retention is still not known. One important point missed in the past analyses is the fact that paper is non-uniform in the plane. In addition to density and thickness mentioned earlier, such properties as porosity, air permeability, fibre orientation etc. also vary in paper on the micro-scale level.

These variations are known to cause drying nonuniformities during the paper manufacturing, especially during convection drying (Gomes et al., 1992; Kiiskinen and Pakarinen, 1998; Hashemi and Douglas, 2001,2003). Such drying nonuniformities may introduce

local strain variations. As convection drying is one of the key features of the heatset offset printing processes, it seems natural to postulate that the drying non-uniformities can cause fluting.

The objective of this study is to propose and examine a fundamental mechanism of fluting formation which is consistent with field observations. Influences of different drying methods are investigated by comparing IR versus convection drying. Retention potential due to ink stiffening is examined both experimentally and numerically.

2. NUMERICAL ANALYSIS OF PAPER WITH MICRO SCALE STRAIN VARIATIONS

A geometrically non-linear finite element analysis was used to simulate local buckling caused by moisture variations during the drying process.

Upon assumed symmetry in the analyses, only a quarter of the web was considered. The web was modelled with an elastic, orthotropic, moisture-dependent material and 4-node fully integrated shell elements (ANSYS, 2005). The elements used the assumed shear strain formulation to alleviate shear locking (Dvorkin and Bathe, 1984). In addition, the method of incompatible modes was employed in formulation, in order to enhance the accuracy in bending-dominated states (Simo and Armero, 1992). The hygroexpansion coefficients were assumed to be 0.05 in the MD and 0.15 in the CD (% deformation/% moisture content change). Moreover, it was assumed that moisture does not cause thickness swelling and also that the moisture is picked up uniformly in the z-direction (thickness direction). The elastic properties were taken from the literature (Land, 2004) and were assumed to be homogeneous. No constraints in the CD were applied since it was assumed that the transport velocity of the web generally diminishes them. Out-of-plane deformations and all rotations were constrained at the right boundary. Also, a constant tension in the MD was applied at the right boundary (Fig. 3). The local strain variations were modelled by introducing randomly distributed round spots with a given moisture difference (Fig. 3). Small numerical perturbations ($10\mu\text{m}$ high bumps) were introduced on the web geometry at these spots.

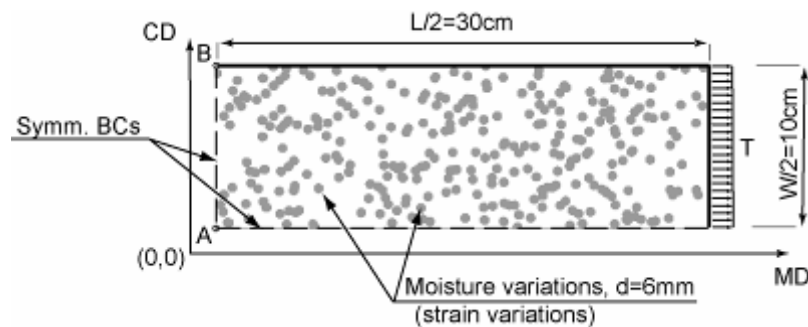


Fig. 3. Randomly distributed moisture difference spots used in the analysis for the reference problem.

For the reference problem the diameter of the spots was chosen to be 6mm and the largest moisture difference examined was 0.8% in moisture content (MC). The following parameters were studied:

- in-plane dimensions
- size of the spots (diameters 3, 6, and 12mm)
- paper basis weight (grammage [g/m^2]/thickness [μm]: 40/32, 60/48, and 80/71)
- tension (100, 200, 400, and 800N/m)
- coverage, i.e., percentage of the total area covered by spots in the area of the specimen (20% and 40%). The fact that spots could overlap was accounted for in calculations of the total area covered by spots.

There are two common methods in integrating the equations of motion, which are usually referred in the literature as explicit and implicit time-integration schemes. Pros and cons of these methods are discussed in details by Dokainish and Subbaraj, (1989) and Subbaraj and Dokainish (1989). Kulachenko et al. (2005) used the explicit technique to analyse a *large* paper web within a reasonable computational time. In this study, however, the effect of the sample size was not found to be important and with a smaller sample (i.e. reduced number of elements), implicit integrations could deliver the solution in a time comparable to an explicit scheme. The main advantage of implicit solution in this study is the ability to track the bifurcation point, i.e. the onset of fluting and relate it with the moisture changes. Computations were performed as transient analyses in which 0.8% moisture difference was gradually being applied during 0.1 second right after the first, steady-state pretension stage. Time-integration effects were considered to be an efficient remedy to prevent the solution from diverging in the vicinity of a bifurcation point. The HHT time integration method (named after the authors' surnames (Hilber et al., 1977)) was used for providing numerical damping in the higher frequency modes. At each time step, the Newton-Raphson iterative process (enhanced with the "Line Search" Method) was performed to solve the non-linear equations. The convergence criterion was based on L2 norms of force, moment and displacement residuals. The transient analysis was followed by the relaxation step with all dynamic effects suppressed.

The distance between two neighbour nodes in the finite element mesh was 0.4mm. A slightly coarser mesh (0.6mm between nodes), although required more Newton-Raphson iterations per load step, did not yield different results for the reference case in terms of wavelength and amplitudes.

3. EXPERIMENTAL MEASUREMENTS OF INK STIFFNESS

In order to evaluate the ink stiffness, a specially designed layout with 400% covered image and non-image areas was printed in a commercial-scale heatset offset printing press on an 80 g/m^2 , $71\mu\text{m}$ thick coated paper. The ink thickness in the image areas was approximately $4\mu\text{m}$ on each side. The bending stiffnesses of the paper strips, cut in the CD from image and non-image areas, were used to estimate the ink stiffness. The bending stiffness was measured in a simple "droop" experiment explained in Appendix.

In this experiment the ink stiffness was estimated to be $\tilde{E} \approx 1.4\text{GPa}$. For the record, the stiffness of the paper in the CD was estimated in this experiment at the level of 2.9GPa , which matched almost exactly the results from the tensile tests on the same paper.

4. FORMATION OF FLUTING

4.1. Factors affecting fluting: Parametric studies

In this simulation the moisture difference was used to create local strain non-uniformity. The geometry of the model, loading and boundary conditions used in the computations are shown in Figure 3 and described earlier. The moisture was increased around the spots. Figure 4 shows a typical numerical analysis result. On the whole, the analyses showed that randomly distributed local moisture variations can cause, rather regular, wavy out-of-plane distortions oriented in the direction of tension. The observed out-of-plane deformations can be characterised as fluting because of the characteristic 1-2cm wavelengths.

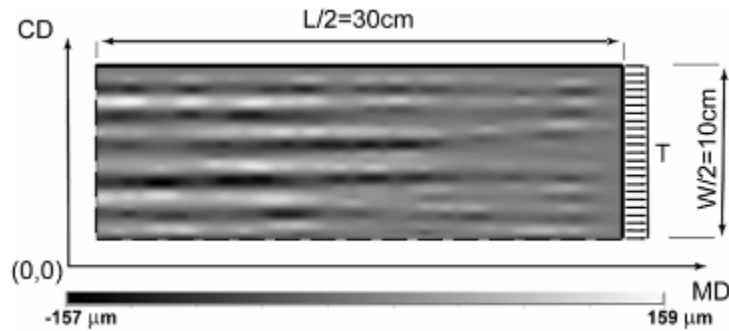


Fig. 4. Out-of-plane deformations due to local moisture variations, the reference case

4.1.1. Influence of specimen size and geometry

Figure 5 shows that the influence of specimen length (L) and width (W) on the wavelength and amplitudes. The results were output from the middle of the web from point A to point B (Fig. 3). Length and width affect the wavelength in a complex way. With higher ratio L/W the amplitudes became larger.

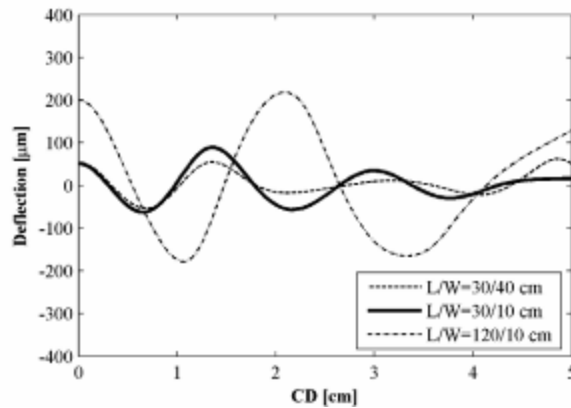


Fig. 5. Comparison of different length/width ratios

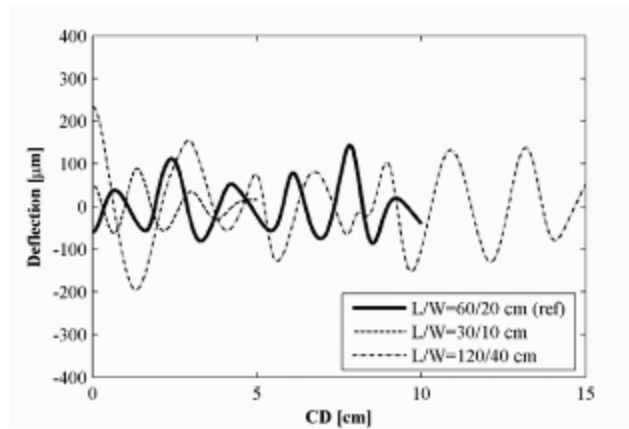


Fig. 6. Effect of proportional scaling

Figure 6 shows the influence of the proportional scaling of the specimen dimensions. The amplitudes increased when the size of the specimen changed from 30x10cm to 60x20cm. The average amplitudes somewhat stabilised however when the sized was increased further to 120x40cm. Based on these results the length and width of the paper sample in the reference problem for the subsequent simulations were chosen to be 60cm and 20cm respectively.

4.1.2. Effects of moisture difference on out-of-plane deformation

Figure 7 shows the dependence of the maximum out-of-plane deflection over the paper sheet on the moisture content difference between the spots and the remaining area of the web. Noticeably, the instability happens abruptly after a certain moisture difference (about 0.4 %). This suggests that buckling occurs only when the magnitude of the moisture variations becomes sufficiently large. This may explain why fluting appears only after some threshold limit of either air impingement velocity or temperature (Mochizuki and Aoyama, 1981; MacPhee et al., 2000).

Both decreasing and increasing the moisture content around the spots resulted in the similar characteristic waviness. The moisture difference needed to cause instability is essentially the same for both cases. Amplitudes and wavelength did not differ much either.

It should be noted that, the contact printing process may also cause non-uniform moisture distribution particularly with paper “unprotected” by coating. This may explain the presence of fluting in SC papers before the dryer (MacPhee et al., 2000).

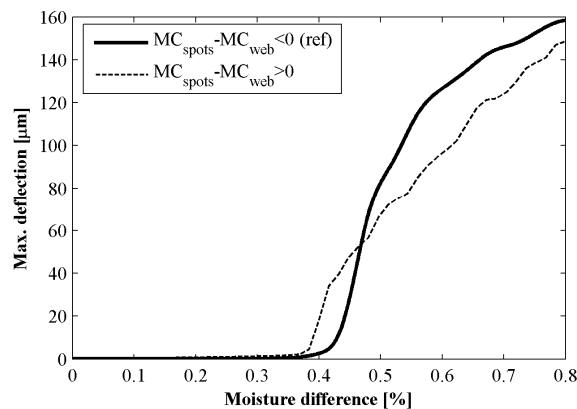


Fig. 7. Parametric study: influence of moisture difference between the spots and the remaining area of the web on maximum deflection

4.1.3. Influence of moisture spots diameter

In this part of the analysis we changed the diameter of the spots as well as their number with the total area covered by moisture spots constant (40% of the sheet area). Figure 8 shows that the diameter of the moisture variation spots clearly influences the wrinkling amplitude. When the diameter is very small (3mm), the waviness pattern is not regular. As the diameter increases, a typical fluting pattern emerges with a certain wavelength. The wavelength was not significantly affected by the diameter of the spots.

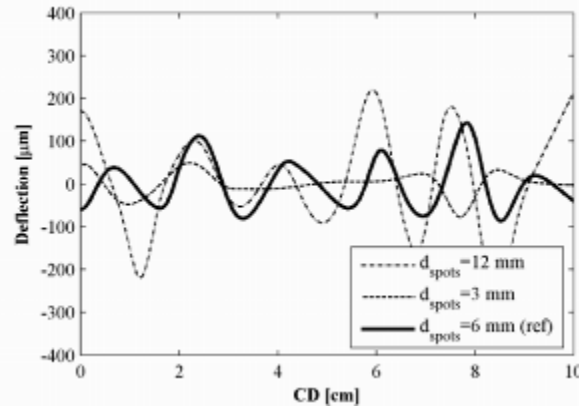


Fig. 8. Parametric study: influence of spot diameter

4.1.4. Influence of percentage of total area covered by spots

Figures 9 and 10 show that less spot coverage creates less distinctive wave pattern. It is worth saying that the same trend is observed when the spot coverage approaches 100%, when the spots cover almost all the paper area. It is also possible to see small bumps developed at the places with imposed moisture difference (Fig. 10). Such bumps in the printed sheets are often referred to as “cockling” and they can also be seen in other cases, for example, in Figure 4, if waviness is filtered out. This suggests that cockling is also originated by the same mechanism as fluting and it is the matter of tension applied in the machine direction and coverage to “transform” cockling into fluting. Cockling will be studied separately in subsequent publications.

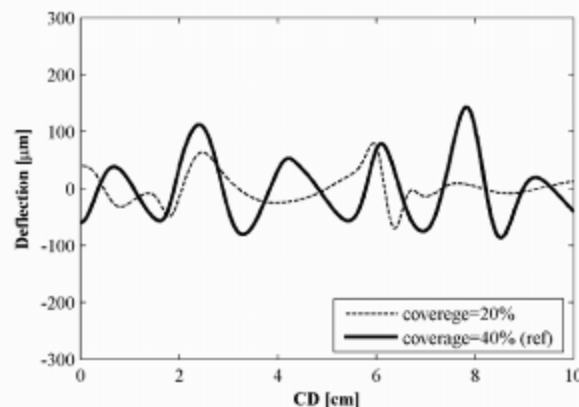


Fig. 9. Parametric study: Influence of percentage of total area covered by spots

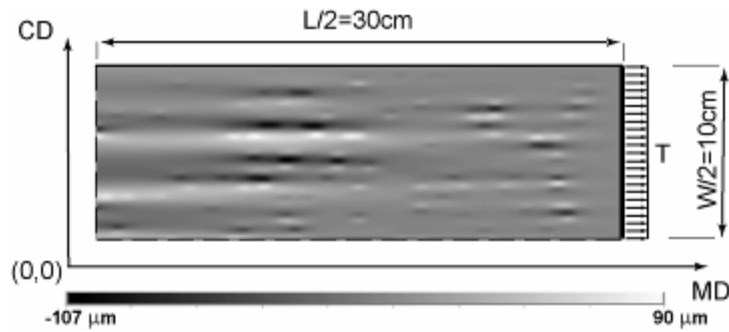


Fig. 10. Out-of-plane deformations due to local moisture variations, reduced spot coverage

4.1.5. Influence of tension

Figure 11 shows the effects of tension on fluting amplitudes and the wavelength. Increasing the tension decreased the amplitudes. This confirms the observation reported by Strong (1984b) for light-weight papers. However, if there is no tension, the waviness obviously does not develop. This means that there is a point at which wrinkling develops and after that the amplitudes start decreasing. At a low tension, the fluting pattern is not regular and the amplitudes are relatively large. On the other hand, within the wide range of tensions from 200N/m to 500N/m, fluting wavelength and amplitudes did not change significantly. This means that small changes in tension within this range will not affect the fluting appearance, as was also observed in the literature (MacPhee, 2000).

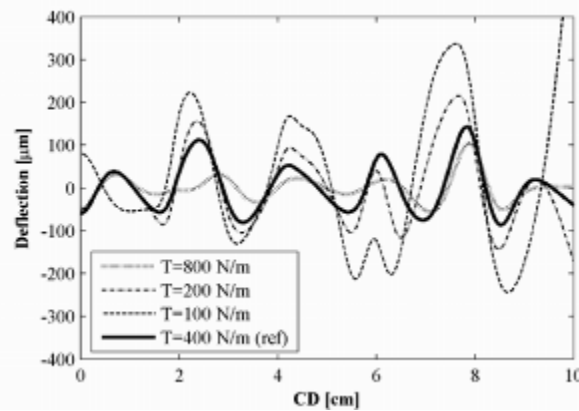


Fig. 11. Parametric study: influence of tension

4.1.6. Influence of paper basis weight (paper thickness, bending stiffness)

Different paper thickness was used to study the effect of the basis weight (grammage). Figure 12 shows that the basis weight of paper influenced the fluting pattern in an expected way, i.e., the greater the thickness (the greater the bending stiffness) the greater the wavelength. This result agrees well with the field observations (MacPhee et al., 2000)

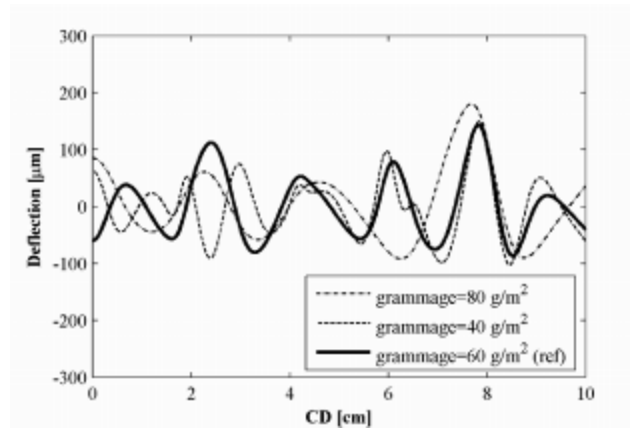


Fig. 12. Parametric study: influence of grammage

Fluting wavelength is one of the key parameters affecting human perception of fluting (Nordström et al., 2002). Table I summarizes the influence of different parameters on wavelengths recorded at the 0.8% moisture difference between the paper and the spots.

Table I. Influence of different parameters on fluting wavelength	
The parameter changed	Wavelength, cm
Reference case (grammage 60 g/m ² , spot diameter 6mm, tension 400N/m)	1.5
Grammage 40 g/m ²	1.2
Grammage 80 g/m ²	2.2
Spot diameter 12mm	1.5
Tension 800N/m	1.6

These results show that grammage (bending stiffness) is the major factor influencing the wavelength.

4.2. Effect of fibre orientation

Variations in fibre orientation are sometimes discussed as a possible reason for out-of-plane distortions in paper (Leppänen et al., 2005). In view of the previous example, it may possibly result in local strain variations needed to create fluting. We decided to study what kind of deformation can occur if a paper sheet possesses non-uniform fibre orientation and, at the same time, is subjected to moistening or drying under tension, i.e. loading conditions which paper experiences during the printing process in a heatset offset press. We considered a paper sheet with the same geometry, boundary conditions and material properties as described in Section 2.

Local variations in fibre orientation for a commercial LWC paper sheet were analysed at VTT Technology. The dimension of the analysed sample was 9cm in the cross direction and 3cm in the machine direction. In this analysis the sample was delaminated to nine thin and transparent layers. Images of the layers were obtained by a desktop scanner and an image analysis was performed. Fibres were distinguished by contrast gradients at the fibre edges. Magnitude and direction of the gradient vectors were examined on 3mm x 3mm cells (Drouin et al., 1996). The result in each layer of the cells was an ellipse-like fibre orientation distribution, from which the orientation parameters such as anisotropy and the fibre orientation angle were

estimated. The anisotropy is calculated as $1 - a/b$ where a and b are the major and minor axes of the ellipse (Fig. 13). The anisotropy affects the material properties such as elastic constants or hygroexpansion coefficients. The fibre orientation angle θ describes the deviation of the major orientation direction from the machine direction.

In the corresponding numerical analysis, the paper was modelled with layered shell. The measured fibre orientation was set as a rotation angle for the corresponding shell layer. These angles θ^i were used to transform the constitutive relations for each of nine layers (Fig. 13).

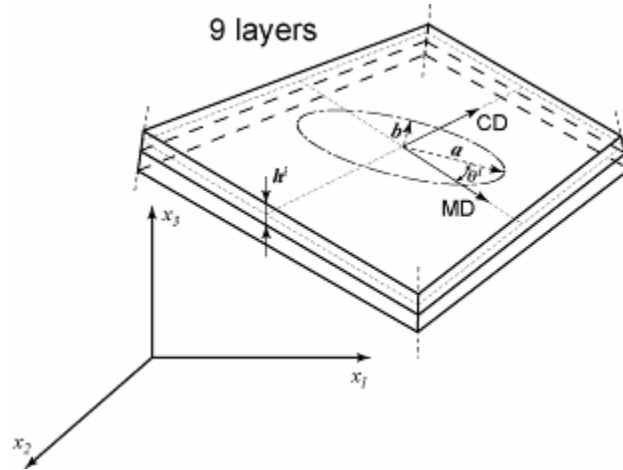


Fig. 13. A layered shell

The anisotropy of the paper generally decreases with increased fibre orientation angle (Fig. 14). It results in a decreased difference between the local material properties, such as elastic modulus and hygroexpansion coefficient, in the MD and CD. In this study we assumed that only the fibre orientation angle varies locally, but the anisotropy remains constant with the value at zero orientation angle (See Fig. 14). It means that the effect of local fibre orientation variations is exaggerated, and therefore the analysis results will represent the worst case scenario in terms of possible effects of fibre orientation upon changing moisture content.

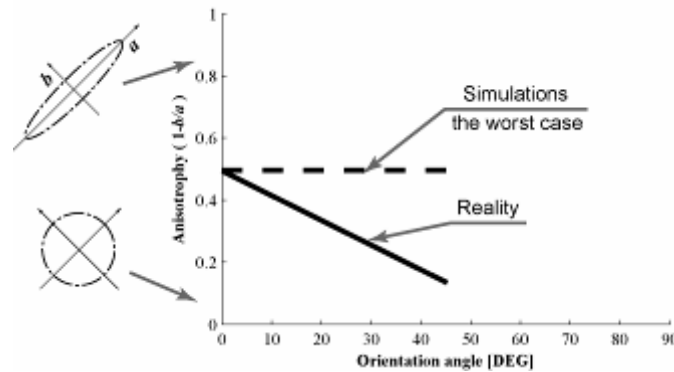


Fig. 14. Dependence of fibre anisotropy on fibre orientation angle.

The size of the sample for the numerical analysis (60cm x 20cm) was larger than the sample from the fibre orientation measurements (3cm x 9cm). In the numerical analyses we “composed” the paper sheet using the measured data in the way shown in Figure 15. Note that such composition helps to circumvent sudden changes in fibre orientation at the “stitches”.

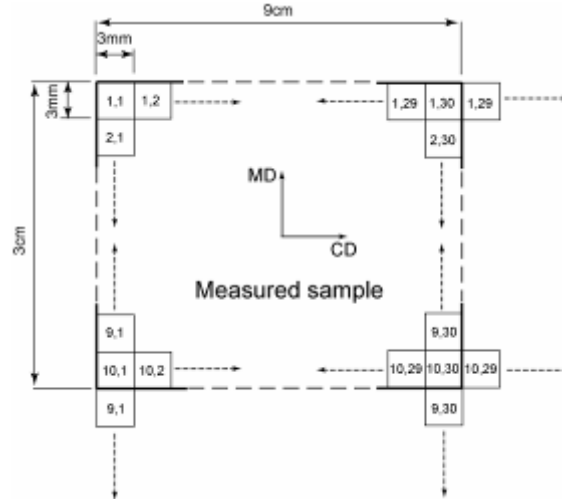


Fig 15. Composition of the paper sheet from measured samples

In the finite element analysis, the no-slip condition was assumed between the element layers. The calculation of interlaminar shear stresses was based on simplifying assumptions of unidirectional, uncoupled bending in each principal direction (bending about one principal direction does not result in a restraining moment about the other directions). It was also assumed that no shear is carried at the top and bottom surfaces of an element. The normal to the middle plane before deformation was assumed to remain straight after deformation (ANSYS, 2005). One integration point per layer thickness was used.

The specimen was pre-stretched with a tension of 400 N/m and moisture was changed uniformly over the area of the specimen. Perturbation bumps were introduced in the same places as in the reference case discussed in Section 2. We modelled the uniform 4% moisture uptake and 4% moisture loss.

Results in Figures 16-18 showed that the local variations of fibre orientation indeed cause waviness, but this waviness does not have much resemblance to fluting in terms of its regularity and wave length. Large deflections at the free edge can be explained by so-called local “curl” due to the two/sidedness, i.e. the fibre orientation angle on one side of the paper was consistently greater than that on the other side.

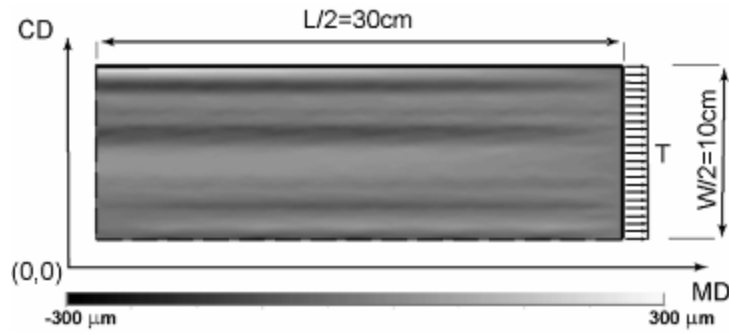


Fig. 16. Distortion due to fibre orientation induced by 4% moisture uptake (a part of the mapped displacement field at a top left corner is out of colour range)

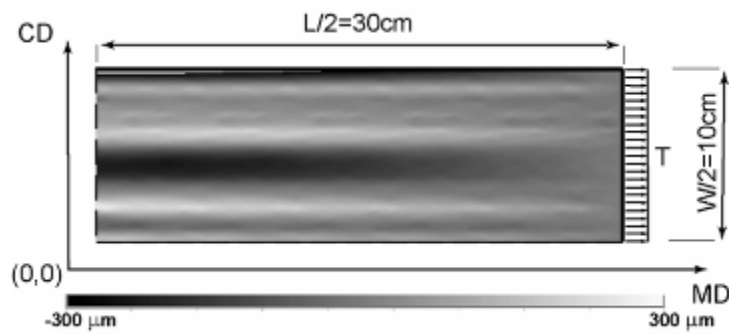


Fig. 17. Distortion due to fibre orientation induced by 4% moisture loss (a part of the mapped displacement field at a top left corner is out of colour range)

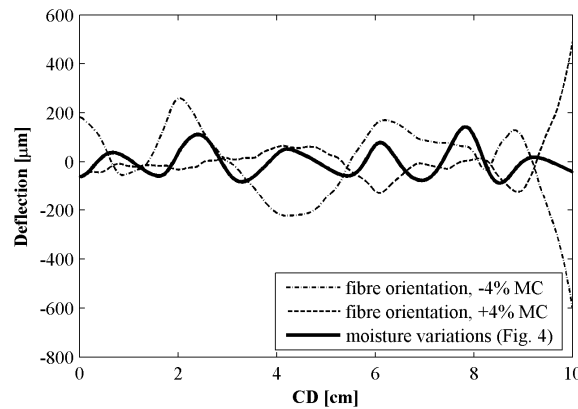


Fig. 18. Distortion induced due to fibre orientation and moisture variations. Comparison along the line AB (Fig. 3).

It should be noted that the explanation of fluting based on this local, in-plane fibre orientation distribution is not consistent with some field observations. For example, fluting propensity of paper is known to be strongly affected by calendering (Waech and Sze, 1996; Begemann, 2005), in which paper is subjected to high pressure in the thickness direction with its fibre orientation constant.

4.3. Effects of drying non-uniformity

Drying methods were indicated as a potential cause of fluting in the literature (Mochizuki and Aoyama, 1981; MacPhee et al., 2000): for example convection drying creates non-uniformity of moisture and thus promotes fluting. In order to confirm the basic effect of drying methods, laboratory-scale experiments were performed.

The main goal of these experiments is to compare the influences of drying methods on the fluting. An SC 60 g/m² paper sheet 70x22cm were cut from the roll, subjected to a high humidity of 90% for 1 hour (to simulate water application during printing) and clamped by two parallel jaws in a tensile tester. It was subjected to a tension of 450N/m which remained constant throughout the experiment. Digital Speckle Photography (DSP, ARAMIS System from GOM mbH) equipment was used to monitor the out-of-plane distortion of the web. Two drying techniques were investigated: IR drying and convection drying. In the case of IR drying, three powerful 2 kW IR lamps were placed behind the web at a distance 15-20cm. It was possible to regulate the amount of heat generated by the dryer. For convection drying we used a powerful 2 kW air blower with exit air temperature up to 150°C. A pistol-type IR temperature sensor was used to measure current paper temperature. In the first trial, paper was steadily dried with the temperature about 80°C (slow IR drying) for about 1 minute. In the second trial the paper was dried at the maximum IR capacity for about 15 seconds (fast IR drying). The paper temperature was quickly raised to about 150-160°C. The air blower was used in the last trial. The hot air was blown from a distance of 5-10cm, starting from the upper part of the paper strip and quickly extended toward the bottom.

IR drying generally provides more uniform moisture removal since there is no convection and only little interactions with paper structures. Heat is applied uniformly all over the web.

In all cases the papers wrinkled, however the appearance of the wrinkles was different. With slower drying the wavelength of wrinkles was relatively high 3-4cm. The wrinkles were present mostly in the middle of the paper strip. After unloading, wrinkles relaxed almost completely.

Fast IR drying changed the wrinkle pattern (Fig 19a). It became irregular, with some local cockling. The dominant, most visible wavelength was still 3-4cm. After unloading most of the out-of-plane distortion relaxed except for the cockling-like deformation.

The air dryer altered the wrinkle appearance drastically (Fig 19b). A regular waviness with the wavelengths of 1-2cm appeared across the whole width. It appeared almost immediately as the heated air was applied. These wrinkles were most reluctant to relax from all three tests. The similar effect with convection drying was observed on thicker LWC paper but with significantly smaller wrinkling amplitudes.

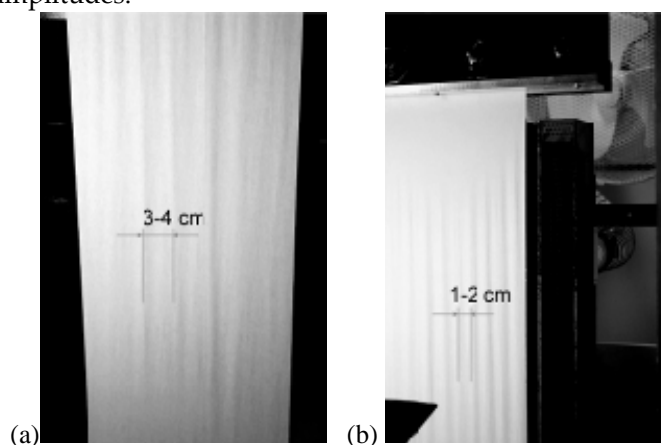


Fig. 19. Appearance of the wrinkles after (a) fast IR drying; (b) convection drying

Figure 20 shows the difference in the wavelength captured by DSP equipment among the different drying methods. This result confirms the field observation concerning influences of drying methods on fluting: convection drying causes fluting. Since convection drying is known for creating local moisture nonuniformities (Gomes et al., 1992; Kiiskinen and Pakarinen, 1998; Hashemi and Douglas, 2001,2003), these results also support our hypothesis of fluting formation.

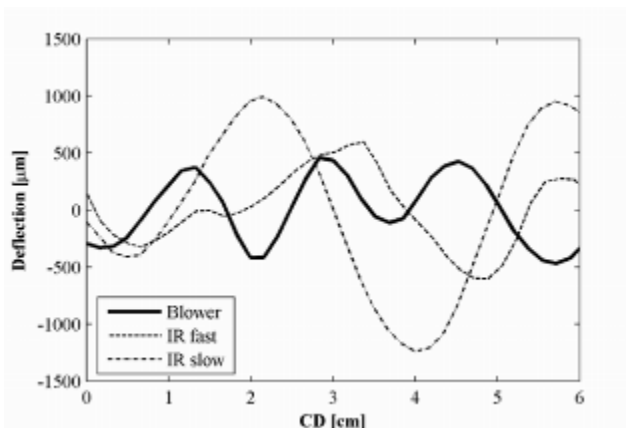


Fig. 20. Measured out-of-plane displacements after different drying methods

4.4. Visualization of air permeation variation in paper

It was shown by Hung (1986) and in this work that although drying is the necessary condition for fluting to occur, it is convection drying which affects fluting the most. Begemann (2005) showed recently that SC paper with higher average permeability has higher fluting tendency if it is calendered online. Meanwhile, fluting propensity of offline calendered papers is generally low and unaffected by average permeability. The most obvious advantage of offline calendering is that most of the moisture variations created during the drying process will even out. Such moisture variations may result in uneven compression during calendering which may create structural variations in the paper, such as permeability variation. Begemann (2005) also reported a reduction in fluting tendency brought by an “overdrying” technique during online calendering. In this case paper is dried extensively, to 2% moisture content, before calendering and then immediately reconditioned by steam showers. Obviously overdrying and re-moisturizing lessens the moisture variations and essentially leads to the same effect as offline calendering. Based on these speculations from the field experience it seems natural to assume that it is the variation in air permeability/porosity that affects the fluting propensity of paper. Naturally, the paper with large variation in air permeability may have moisture variations during through air drying.

We decided to investigate the scale of permeability variations and find out whether there is a difference in a paper known to be prone to fluting and cockling and in a paper with relatively low fluting tendency. As was demonstrated, the scale of moisture variation would play the crucial role in fluting formation.

We used two hollow cylinders (Fig. 21). The pressure inside the outer cylinder moves the inner cylinder upwards until it reaches the fixation ring.

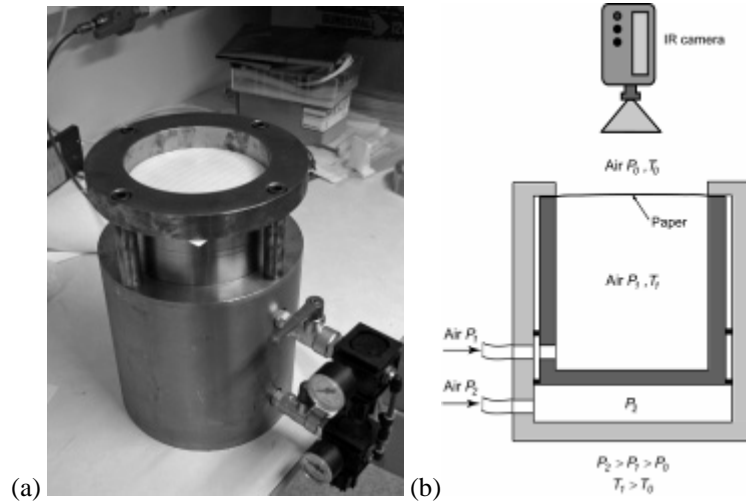


Fig. 21. Experimental setup for permeability testing

A paper is placed on the top of the inner cylinder and it was sealed by the upper ring. The pressure inside the cylinders was controlled by two separate pressure regulators. The air was pumped into the inner cylinder through the small hole in the bottom and redirected toward the walls.

In this experiment the ambient room temperature was about $T_o = 22^\circ\text{C}$. The cylinders were heated to approximately 40°C so that when the paper was fixed, its temperature stabilised near 30°C (with slightly higher temperature at the edges where it contacts the fixation ring). The temperature of the air pumped into the inner cylinder was 20°C but the air temperature raised inside preheated inner cylinder to approximately $T_1 = 25^\circ\text{C}$. The pressure inside the inner cylinder was increased which created a constant air flow through the paper sample. An IR camera was placed above the paper to monitor the temperature changes (Fig. 21b).

Two uncoated papers were investigated. P1 is known for cockling and fluting tendency and P2 is known to have a relatively low fluting propensity and without cockling. Figure 22 (upper row) shows the initial in-plane temperature variation in the paper before the air pressure was changed. The temperature varied globally and the paper had a higher temperature toward the outer boundary because of the heated cylinder. As soon as the pressure was changed, local temperature variations emerged on 1 cm scale (Fig. 22, middle row). Since such variations could be seen for a long period of time in the same spots and disappeared as soon as the air flow was removed we assumed that they indicated the local air permeability variations in paper. A bandpass filter was applied onto measured temperature variations to remove the global temperature variations and noise (Fig. 22, bottom row). We filtered out large structures down to 1 cm and small structures up to 1 mm. We processed the images further adjusting the colour balance until the mean gray value became 128 (on the scale 0 to 255). We calculated the coefficient of variation (COV) by dividing the standard deviation (taken from the histogram) onto the mean value (128). We distinguished the variations by filling the area having gray value from 126 to 130 with black colour.

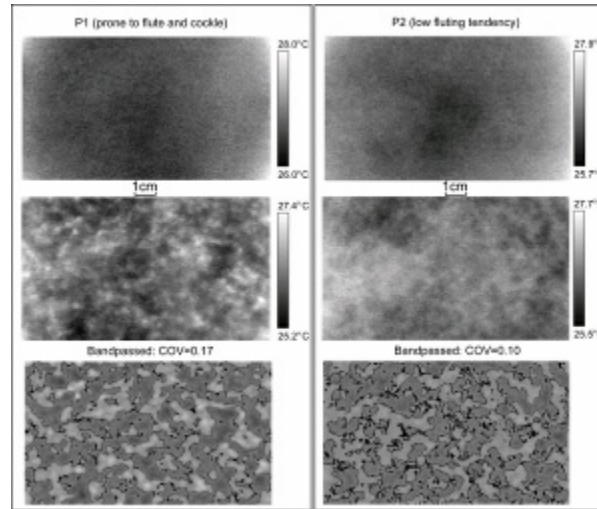


Fig. 22. In-plane temperature variations captured by IR camera equipment: before the pressure change (upper row), after the pressure change (middle row) and bandpassed (bottom row).

There were two important observations made during this experiment. There are observable permeability variations on a 1cm scale. It is the scale needed to create a fluting pattern according to the numerical experiment reported earlier. The second observation was that paper P1 known for high fluting tendency had more variation in permeability than the paper P2 known for moderate fluting tendency. In terms of statistical values, the coefficient of variation (COV) was 0.17 for P1 and 0.10 for P2.

This again suggests that variations in permeability on a 1cm scale are *the key factor* influencing the fluting tendency.

5. FLUTING RETENTION

5.1. Numerical analysis

Several authors (Habeger, 1993; Hirabayashi et al., 1998; Coffin, 2003) proposed that stiffening of the ink during drying fixes the shape of fluting. We examined this hypothesis first by numerical analyses.

In order to model the ink, two shell sets sharing the same nodes were introduced in the image areas of the finite element model. The first shell set is to represent the paper material. The second shell set consists of layered shells with the middle layer that had a “dummy” material assigned with negligibly small elastic modulus. The top and bottom layers represent the ink and have the measured ink stiffness (Fig. 23).

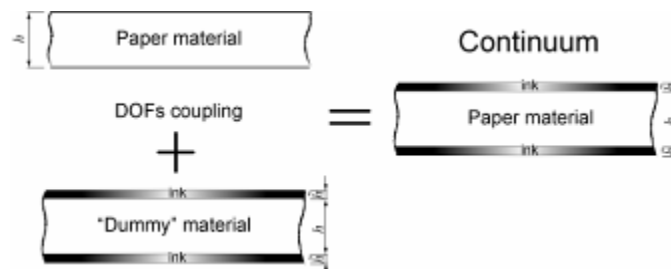


Fig. 23. Ink modelling principle

During the moisture change the ink elements were disabled by assigning very small stiffness values and therefore they followed the deformation of the paper web without resistance. At the end of the drying stage the ink elements were *enabled* with zero-strain state corresponding to the deformed configuration of the web after the moisture change. This situation obviously represents the worst-case scenario in terms of solidification and gives the upper bound of ink retention potential.

Fluting retention was modelled with 4 different ink thicknesses. Elastic, orthotropic, moisture-dependent material properties reported by Land (2004) for 71 g/m^2 coated paper were used in the simulations. The paper thickness was set to be $71 \mu\text{m}$ in order to match 80 g/m^2 paper used in the printing trial. The tension was 171 N/m . Ink was introduced in the area shown in Figure 24.

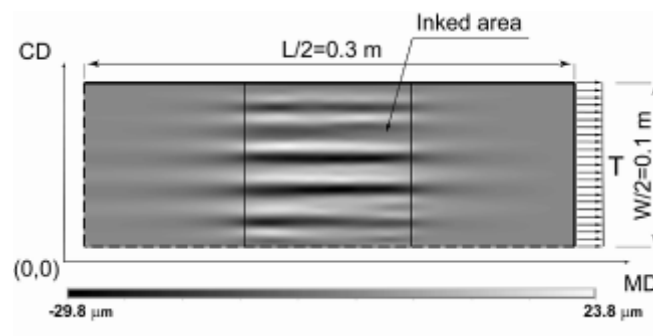


Fig. 24. Deformation under tension after moisture reconditioning (one quarter of the sheet is shown)

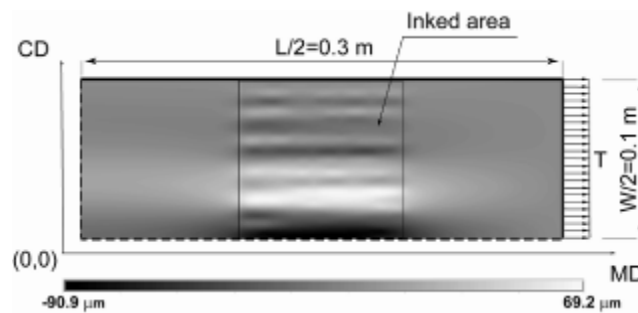


Fig. 25. Deformation "without" tension after moisture reconditioning

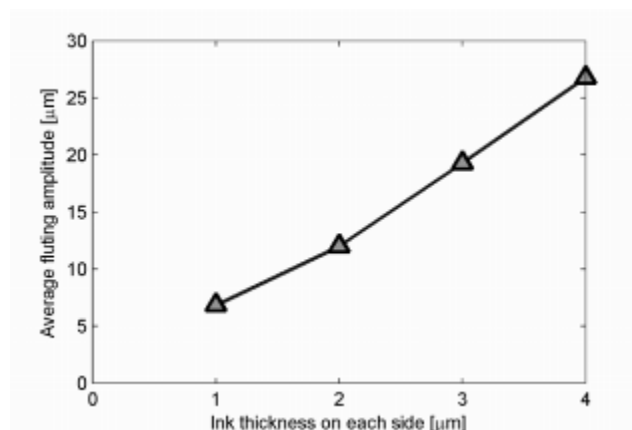


Fig. 26. Influence of ink on fluting retention

The ink was activated on the deformed shape after increasing the moisture around the spots. The sample was unloaded to the minimum tension ($\sim 1\text{N/m}$ needed to maintain numerical stability). The residual fluting patterns after moisture reconditioning are shown in Figure 24 (before unloading) and in Figure 25 (after unloading). As seen in these figures, most of the distortion disappears after unloading.

The average fluting amplitude after moisture reconditioning, but before unloading, was calculated. Results (Fig. 26) showed that even with the assumption that ink solidifies on the deformed shape (upper bound estimate), the fluting amplitudes were rather low ($25\text{-}30\mu\text{m}$) as compared with typical fluting amplitudes ($100\text{-}150\mu\text{m}$) even for a very thick ink layer ($4\mu\text{m}$). Moreover, after unloading the fluting amplitudes *further* decreased and new waves with higher wavelength emerged (Fig. 25). This implies that fluting retention due to ink stiffening is limited.

5.2. Experimental analysis

Printed samples from the commercial scale print trial were analysed to identify fluting wavelengths and amplitudes and to monitor the fluting relaxations after a prolonged period of time.

The FRT MicroProf equipment was used to analyze the out-of-plane deformations of the paper. Using the CHR 150 optical sensor, the sample is illuminated by a focused white light. An internal, passive optical system, using chromatic aberration, splits the white light into different colours (corresponding to different wavelengths). A miniaturised spectrometer detects the colour of the light reflected by the sample and determines the position of the focus point, and, by means of an internal calibration table, the vertical position of the sample surface. Figure 27 schematically shows how the MicroProf equipment functions.

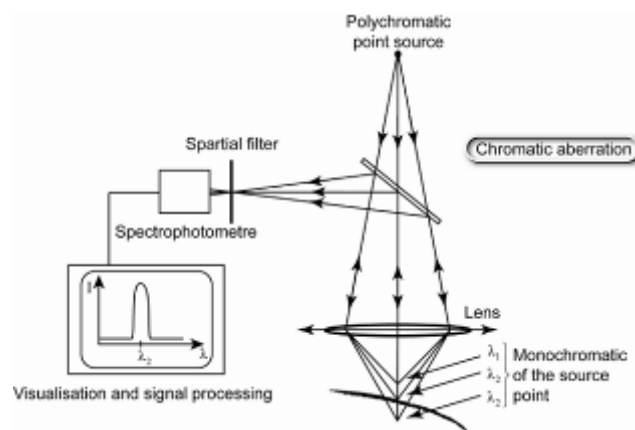


Fig. 27. FRT MicroProf measurement principle

Image and non-image areas were scanned and processed after 2 weeks and 3 months later of the trial. Original scans contained different wavelengths. Higher wavelength could represent residual tension wrinkle which is not usually seen in a printed sheet. Our analyses (Kulachenko et al., 2005) and field observation show that tension wrinkling and fluting may superimpose and not necessarily interact (Fig. 28).

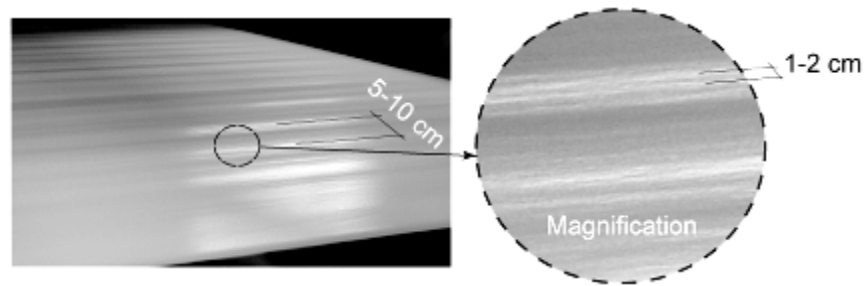


Fig. 28. Tension wrinkles and fluting on the paper web after the drying section in a commercial scale printing press.

Therefore, the high pass FFT filter was applied onto the scanned data to extract the fluting pattern with wavelengths of approximately 2cm. It is worth mentioning that the waves with much higher wavelengths are not generally perceived by the eye. Original and filtered data are shown in Figures 29,30.

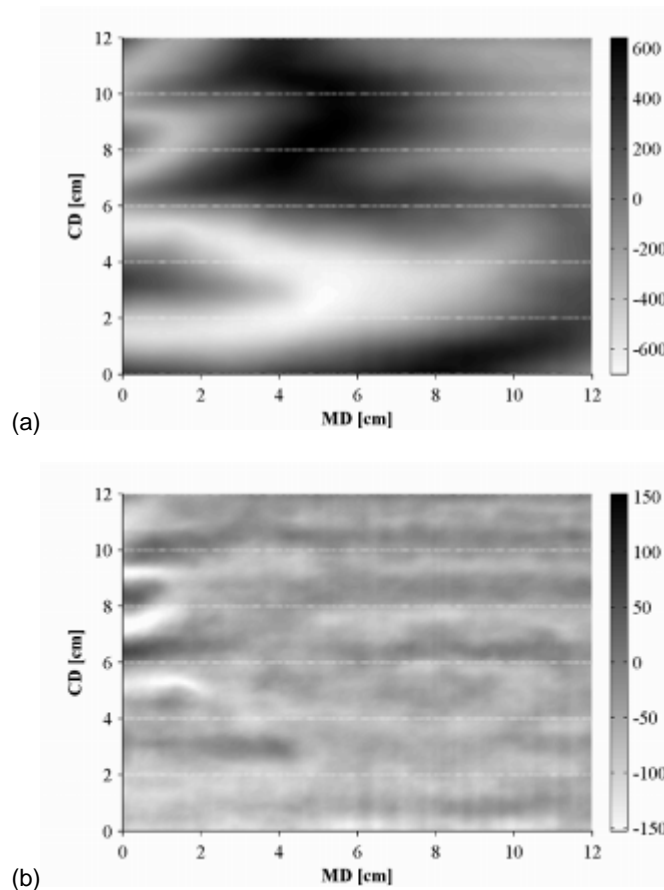


Fig. 29. Surface distortion in the non-image areas shortly after the trial: (a) unfiltered; (b) filtered

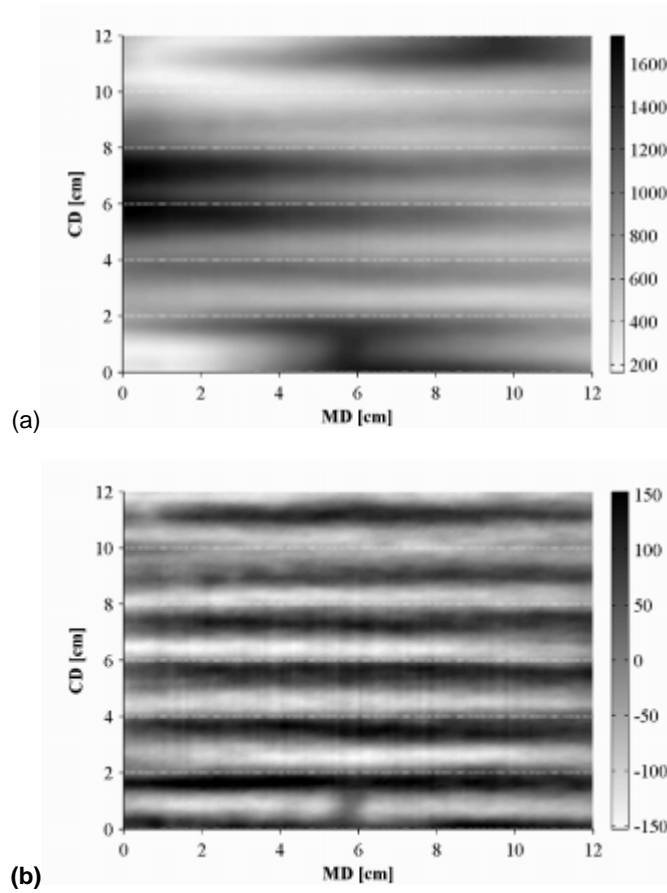


Fig. 30. Surface distortion in the image areas shortly after the trial: (a) unfiltered; (b) filtered

The wavelength of the flutes in the printed areas was about 2cm and the amplitudes were about $150\mu\text{m}$, which is much greater than numerically estimated ($30\mu\text{m}$) based on the ink stiffening hypothesis. The unprinted area has out-of-plane distortions of smaller amplitudes and less distinctive wave pattern (Fig. 31a). The same paper sheet was analysed again 3 months after the trial (Fig. 31b). Clearly fluting did not relax under this condition.

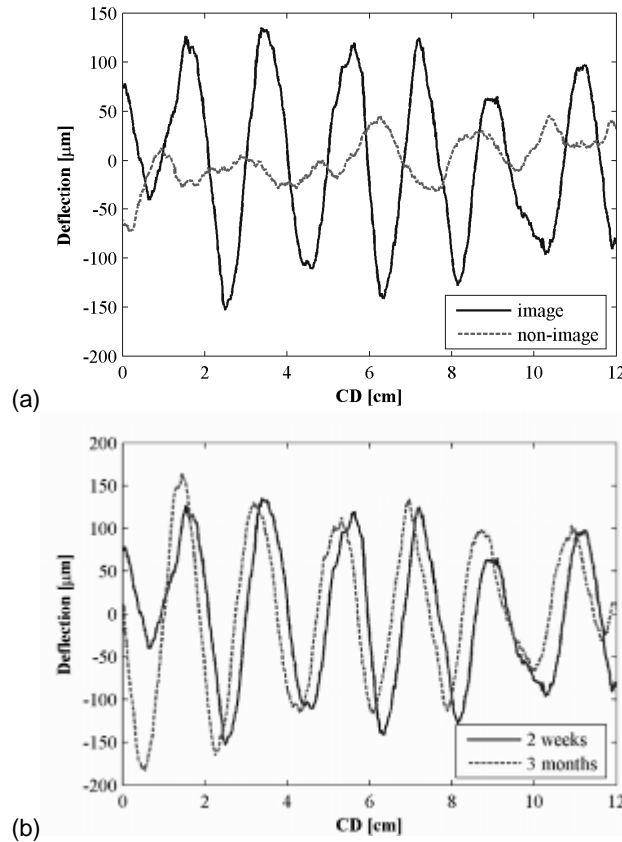


Fig. 31. Residual fluting: (a) in the image and non-image areas; (b) in the printed areas after 2 weeks and 3 months.

Therefore, these experimental results showed that the magnitude of fluting is much higher than that predicted from the ink-stiffening hypothesis. This poses a new question: what retains fluting.

5.3. Effect of temperature on residual deformation in paper

The fact that fluting remains predominantly in the image areas suggests two important factors. First, more water is generally applied onto the image areas during printing and is evaporated during drying. This will increase the chances of developing more irreversible shrinkage in the printed areas after drying and reconditioning. Second, the image areas attract more heat during drying (Hung, 1986; MacPhee et al., 2000): the web has significantly higher temperature in image areas (60°C) than in non-image areas (30°C) after the chill roll.

In general, the temperature of the paper in a commercial heat-set web offset dryer may range from 110 to 150°C. In order to study the effect of temperature on residual deformation in paper the following test was carried out. An initially flat 10 cm long paper strip was rolled and fit into a metal pipe of 3 cm in diameter. The reference sample (LWC paper, 60 g/m²) was dried by desorption at room temperature. This reference strip was then reconditioned. Several other strips were also rolled into the pipes and placed into a convection oven so that hot air goes straight through the tubes (Fig. 32). The air temperature was gradually being increased from

20°C and the specimens were taken out from the oven at different temperatures (90°C, 115°C, 125°C, 130°C, 140°C, 145°C).

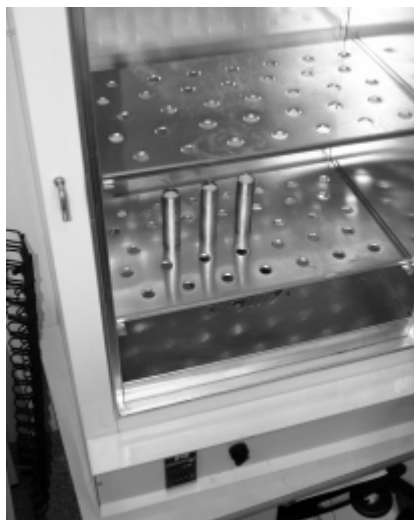


Fig. 32. Convection oven used to dry the paper inside the tubes

Since paper stayed in the convection oven for sufficiently long time (more than 1min) at a high temperature, we assumed that water was completely removed from all the strips during drying. All strips were reconditioned after being released from the pipes. Figure 33 shows the residual curvatures in the strips one day after the trial. The effect is obvious, the higher the temperature, the higher the curvature. Higher temperature clearly induced greater plastic deformation in paper.

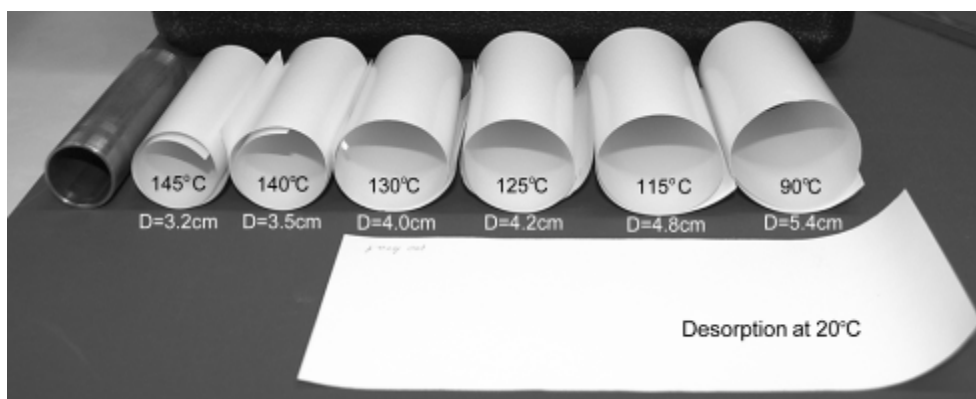


Fig. 33. Comparison of residual curvature in papers samples released from the oven at different temperature to that in the reference paper sample dried by desorption. D denotes the residual diameter after reconditioning.

6. CONCLUSION

Small scale strain variations, such as caused by in-plane moisture variations, could produce wrinkles that have a close resemblance to fluting in terms of wavelength (1-2cm). The occurrence of such wrinkles depends on the size and distribution of the micro-variations, as well as the local difference in moisture content. Numerically, the local moisture difference was within a very plausible range that may be encountered in the realistic heatset printing processes.

The hypothesis proposed here consistent with the experimental results: faster convection drying, which involves interactions with non-uniform paper structures, created the wrinkle wavelengths similar to fluting, in contrast to IR drying. The proposed mechanism also explains, at least qualitatively, many of the field observations, e.g., fluting is less of an issue for slower presses with moderate drying rate.

Ink stiffening due to drying was found to be insufficient to retain fluting, even in the extreme case of 400% coverage. It was shown, on the other hand, that high drying temperatures promote inelastic (irreversible) deformations in paper and this may itself preserve fluting. The fact that image areas usually have higher temperatures after drying (i.e. attract more heat) explains why residual fluting predominantly retained in the printed parts of the sheet.

ACKNOWLEDGEMENTS

The financial support of T2F printing research programme is greatly acknowledged. The help in experimental part of the work, provided by SCA Packaging Research in Sundsvall, Sweden and particularly by Bo Westerlind is also greatly appreciated.

APPENDIX: ESTIMATE OF INK STIFFNESS BY DROOP TEST

Let us consider a narrow paper strip bent under self-weight in a coordinate system with the x-axis directed in the length direction (Fig. A1).

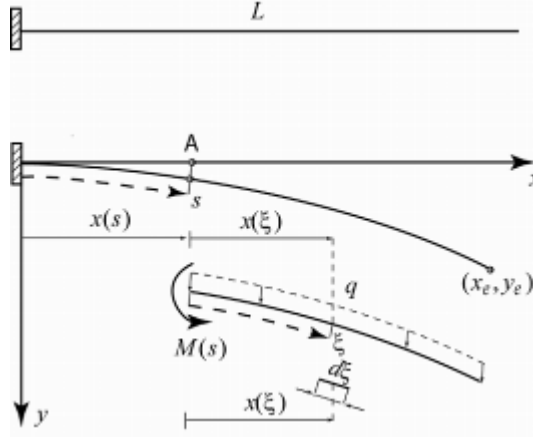


Fig. A1. Problem representation

The bending moment M at a point A of the strip can be written as follows

$$\begin{aligned} M &= \int_s^L q(x(\xi) - x(s)) d\xi \\ &= q \int_s^L x(\xi) d\xi - qx(s) \int_s^L d\xi = q \int_s^L x(\xi) d\xi - qx(s)(L-s) \end{aligned} \quad (\text{A.1})$$

where s and ξ are the curvilinear coordinates, q is the distributed weight; L is the length of the strip.

The moment M can be related to the curvature κ as follows:

$$M = D\kappa = D \frac{d\varphi}{ds} = q \int_s^L x(\xi) d\xi - qx(s)(L-s) \quad (\text{A.2})$$

where φ is the slope angle and D is the bending stiffness. After differentiating with respect to s we receive

$$\begin{aligned} D \frac{d^2\varphi}{ds^2} &= -qx(s) - q \left(\frac{dx}{ds} L - x(s) - s \frac{dx}{ds} \right) \\ &= -q \frac{dx}{ds} (L-s) \end{aligned} \quad (\text{A.3})$$

Additional equations based on geometrical considerations are:

$$\frac{dx}{ds} = \cos \varphi \quad \frac{dy}{ds} = \sin \varphi \quad (\text{A.4})$$

The boundary conditions can be written as follows

$$\begin{aligned} y(0) &= 0 & x(0) &= 0 \\ \varphi(0) &= 0 & \frac{\partial \varphi}{\partial s}(L) &= 0 \end{aligned} \quad (\text{A.5})$$

Equations (A.3)-(A.5) represent a non-linear boundary value problem. By solving these equations with different values of D , we can eventually find the bending stiffness so that $x(L) = x_e$ and $y(L) = y_e$ where x_e and y_e are the coordinates of the free end measured in the experimental setup (Fig. A1). The number of tested stripes was 40 (20 printed and 20 unprinted). The grammage, paper thickness and deflection in the droop test were measured for each individual paper strip. The bending stiffness D was fitted in a numerical procedure so that the resulting coordinates x_e and y_e matched those from the experiment.

We assume that the strain varies linearly along the normal to the paper middle surface:

$$\gamma = \varepsilon + y\kappa \quad (\text{A.6})$$

where ε is the membrane strain in the middle plane $y = 0$. If the response of the shell is linear elastic, we may write the stress along the shell normal as:

$$\sigma(y) = E(y)(\varepsilon + y\kappa) \quad (\text{A.7})$$

where $E(y)$ is the elastic stiffness. We assume that transverse effects are negligible and the ink layer is present on both sides of the strip. The moment M can be expressed as follows:

$$\begin{aligned} M &= \int_{-(h/2+\tilde{h})}^{-h/2+\tilde{h}} b\sigma(y)ydy = 2\kappa b \left[\int_0^{h/2} Ey^2dy + \int_{h/2}^{h/2+\tilde{h}} \tilde{E}y^2dy \right] \\ &= \kappa b \left[E \frac{h^3}{12} + \tilde{E} \frac{\tilde{h}(3h^2 + 6h\tilde{h} + 4\tilde{h}^2)}{6} \right] \\ &= \kappa \left[D + b\tilde{E} \frac{\tilde{h}(3h^2 + 6h\tilde{h} + 4\tilde{h}^2)}{6} \right] \end{aligned} \quad (\text{A.8})$$

where h is the paper thickness, \tilde{h} is the ink thickness, b is the width of the paper sample, E and \tilde{E} are the stiffnesses of paper and ink respectively, D is the bending stiffness of the paper without the ink layer.

Let us denote the bending stiffness of paper with the ink layer \hat{D} as

$$\hat{D} = \left[D + b\tilde{E} \frac{\tilde{h}(3h^2 + 6h\tilde{h} + 4\tilde{h}^2)}{6} \right] \quad (\text{A.9})$$

Using the fact that $\tilde{h} \ll h$, the ink stiffness can be found from known bending stiffness as

$$\tilde{E} \approx \left[\hat{D} - D \right] \frac{2}{\tilde{h}h^2} \quad (\text{A.10})$$

where \hat{D} is taken from the measurements on a strip from image areas and D is from a strip from non-image areas of the same paper sheet.

REFERENCES

- ANSYS, 2005. Theory Reference. Ansys Inc., Southpointe, USA.
- Begemann, U., 2005. Ausgewählte Aspekte der Be- und Verdruckbarkeit aus Sicht des Papiermaschinen-Lieferanten. *Int. Papwirtsch* 3, 36-44, in German.
- Coffin, D., 2003. A buckling analysis corresponding to the fluting of lightweight coated webs. In: *Proc. International Paper Physics Conference*, Victoria, B.C., Canada, 31-36.
- Dokainish, M.A., Subbaraj, K.A., 1989. A survey of direct time-integration methods in computational structural dynamics-I. Explicit methods. *Computers and Structures* 32, 1371-1386.
- Drouin, B., Gagnon, R., Silvy, J., Schroder, A., Butel, M., 1996. High resolution fibre orientation and basis weight measurement. *Journal of Pulp and Paper Science* 22, 237-241.
- Dvorkin, E.N., Bathe, K.J., 1984. A continuum mechanics based four-node shell element for general nonlinear analysis. *Engineering Computations* 1, 77-88.
- Falter, K.A., Schmitt, U., 1987. Influence of heat-effects in web offset printing on strength properties of the paper and on waviness of the print. In: *Proc. 19th International Conference of Printing Research Institutes*, Eisenstadt, Austria, 176-185.
- Gomes, V.G., Crotogino, R.H., Douglas, W.J.M., 1992. The role of local nonuniformity in through drying of paper. In: *Proc. 8th International Drying Symposium*, Montréal, Canada, 994-1003.
- Habeger, C.C., 1993. Tension wrinkling and the fluting of light-weight coated papers in web-offset printing. *Journal of Pulp and Paper Science* 19, 214-218.
- Hashemi, S.J., Douglas, W.J.M., 2001. Paper drying: A strategy for higher machine speed. 1. Through air drying for hybrid dryer section. *Drying Technology* 19, 2487-2507.
- Hashemi, S.J., Douglas, W.J.M., 2003. Moisture non-uniformity in drying paper: Measurement and relation to process parameters. *Drying Technology* 21, 329-347.
- Hilber, H.M., Hughes, T.J.R., Taylor, R.L., 1977. Improved numerical dissipation for time integration algorithm in structural dynamics. *Earthquake Engineering and Structural Dynamics* 5, 283.
- Hirabayashi, T., Fujiwara, S., Fukui, T., 1998. Factors of the fluting of coated paper in web-offset printing. In: *Proc. 1998 Pan-Pacific and International Printing and Graphic Arts Conference*, Montréal, Canada, 52-57.
- Hirabayashi, T., Fujiwara, S., Fukui, T., Suzuki, Y., Tani, Y., Watanabe, D., 2005. Development of new printing paper called OK Non-Wrinkle. In: *Proc. PTS Coating Symposium*, Baden-Baden, Germany, 14.11-14.18.
- Hung, J.Y., 1984. Paper fluting -results of TEC studies. TEC Systems, DePere, Wisconsin, USA.
- Hung, J.Y., 1986. Paper fluting - results of TEC studies. Phase II. TEC Systems, DePere, Wisconsin, USA.
- Kiiskinen, H.T., Pakarinen, P.I., 1998. Infrared thermography at examination of paper structure. *Proceedings of SPIE - The International Society for Optical Engineering* 3361, 228-233.
- Kulachenko, A., Gradin, P., Uesaka, T., 2005. Tension Wrinkling and Fluting in Heatset Web Offset Printing Process, Post-Buckling Analyses, in: I'Anson, S.J. (Eds.), *Advances in Paper Science and Technology*. The Pulp and Paper Fundamental Research Society, Lancashire, UK, pp. 1075-1099.

- Kulachenko, A., Gradin, P., Uesaka, T., 2006. Basic mechanisms of fluting. In: Proc. 92nd Annual Meeting of the Pulp and Paper Technical Association of Canada, Montréal, Canada, A161-A174.
- Land, C., 2004. Effect of moisture amount on HSWO waviness. In: Proc. International Printing and Graphic Arts Conference, Vancouver, Canada, 29-33.
- Leppäanen, T., Sorvari, J., Erkkilä, A.-L., Hämäläinen, J., 2005. Mathematical modelling of moisture induced out-of-plane deformation of a paper sheet. *Modelling and Simulation in Material Science and Engineering* 13, 841-850.
- MacPhee, J., Bellini, V., Blom, B.E., Cieri, A.D., Pinzone, V., Potter, R.S., 2000. The effect of certain variables on fluting in heatset web offset printing. Web Offset Association, Affiliate of Printing Industries of America Inc.
- Mochizuki, S., Aoyama, J., 1981. Effects of fast ink drying conditions on multi-colored moving web. *TAGA Proceedings*, 43-55.
- Mochizuki, S., Aoyama, J., 1982. Multi-colored moving Web (II). *TAGA Proceedings*, 483-496.
- Nordström, J.E., Linberg, S., Lundström, A., 2002. Human perception and optical measurement of HSWO waviness. In: Proc. International Printing and Graphics Arts Conference, Bordeaux, France.
- Simmons, S., Blom, B., Dreher, C., Dewildt, D., Coffin, D., 2001. Parametric evaluation of web offset fluting. In: Proc. TAGA'S 53rd Annual Technical Conference, San Diego, CA, USA, 162-185.
- Simo, J.C., Armero, F., 1992. Geometrically nonlinear enhanced strain mixed methods and the method of incompatible modes. *International Journal for Numerical Methods in Engineering* 33, 1413-1449.
- Strong, W., 1984a. Paper distortion from heatset web offset printing. *Graphics Arts Bulletin* No. 11, Mead Corp.
- Strong, W., 1984b. A study of fluting in coated papers printed by blanket-to-blanket offset presses. In: Proc. GATF Technical Forum, Chicago, USA, 20.21-20.32.
- Subbaraj, K.A., Dokainish, M.A., 1989. A survey of direct time-integration methods in computational structural dynamics-II. Implicit methods. *Computers and Structures* 32, 1387-1401.
- Waech, T.G., Sze, D.H., 1996. Predicting the fluting tendency of light weight coated paper. In: Proc. 1996 International Printing and Graphic Arts Conference, Minneapolis, USA, 65-73.